

IMECE 2002-34273

NESTED OPTIMIZATION OF AN ELEVATOR AND ITS GAIN-SCHEDULED LQG CONTROLLER

Hosam K. Fathy¹, Scott A. Bortoff², G. Scott Copeland², Panos Y. Papalambros³ and A. Galip Ulsoy³

ABSTRACT

This paper studies the combined optimization of an elevator's design (plant) and LQG controller for ride comfort. Elevator dynamics and primary vibration sources (drive motor torque ripple and guide rail irregularity) are modeled using an object-oriented language. The resulting model is nonlinear. Elevator vibrations are minimized with respect to both the design and the LQG controller. LQG gains are scheduled versus cab mass and height for robustness. Sequential plant/control optimization produces an optimal ride only when the torque ripple is the dominant disturbance. Otherwise, passive vibration reduction decreases the controller's authority over the vibrations, hence coupling the plant and control optimization problems. Combined plant/controller optimization, using a nested strategy, mitigates this coupling and finds the correct optimal system design.

1. INTRODUCTION

Maximizing elevator ride comfort increases in difficulty as travel speeds and passenger cab compliances increase. Therefore, sequentially optimizing an elevator's open-loop plant first and then its controller is becoming increasingly inadequate for this task. Research in several fields has shown that sequential optimization does not furnish truly optimal system designs because it fails to account for the effect of a plant's design on its ease of control [1-6]. To design a truly optimal system, its plant and controller must be optimized simultaneously [1-3]. This paper shows that simultaneously optimizing an elevator's plant and controller yields a truly optimal ride unattainable using sequential optimization.

Unlike most models in the combined plant/controller optimization literature, an elevator's dynamic model is not linear and time-invariant (LTI), but rather dependent on the cab height (a state variable) and mass (an exogenous variable) and hence nonlinear. This paper extends previous combined optimization strategies to problems where the control is adaptive rather than LTI and uses the resulting theory for elevator ride comfort maximization.

Physically, improving an elevator's ride quality involves optimizing either its plant or control to isolate the passenger cab from two main disturbances: the drive motor torque ripple and the guide rail irregularity. These two isolation means compete because passive vibration isolation reduces the controller's authority over the vibrations. Combined optimization accounts for this competition, or coupling, thereby producing a truly optimal elevator system.

TABLE 1: NOMENCLATURE

$a \in \mathbf{H}, C_a \in \mathbf{R}^{1 \times n_z}$	Passenger acceleration & matrix relating it to states.
$\mathbf{A} \in \mathbf{R}^{n_z \times n_z}, \mathbf{B} \in \mathbf{R}^{n_z \times n_u},$ $\mathbf{G} \in \mathbf{R}^{n_z \times n_w}, \mathbf{C} \in \mathbf{R}^{n_y \times n_z}$ and $\mathbf{D} \in \mathbf{R}^{n_y \times n_u}$	Matrices of reduced-index linearized model.
E	Expectation operator.
$\mathbf{E}_w \in \mathbf{R}^{n_w \times n_w}, \mathbf{E}_v \in \mathbf{R}^{n_v \times n_v}$	Disturbance and noise covariances.
f	System optimization objective (same as J), expressed explicitly in terms of \mathbf{x}, \mathbf{x}_e and \mathbf{z}_r^o .
$\mathbf{f}_z, \mathbf{g}_z, \mathbf{g}_y$	State, state constraint & output equations
$\mathbf{f}_{zr}, \mathbf{g}_{yr}$	Reduced-index state and output equations.
$\mathbf{g} \in \mathbf{R}^3$	Acceleration of gravity.
\mathbf{H}	<i>Hilbert</i> space of all scalar real functions of time.
$J \in \mathbf{R}$	System optimization objective.
$\mathbf{K} \in \mathbf{R}^{n_u \times n_z}, \mathbf{L} \in \mathbf{R}^{n_z \times n_y}$	LQG feedback and estimation gains.
$L \in \mathbf{R}$	Length of a given rope segment.
$n_z, n_u, n_w, n_v, n_y, n_{xp}, n_{xe}$	Integer numbers of states, inputs, disturbances, noises, outputs plant design variables and exogenous variables.
\mathbf{R}	Set of real numbers.
$R \in \mathbf{R}$	Control weight in objective function.
$\mathbf{s} \in \mathbf{R}^3$	Unit vector along a given straight rope segment.
$t \in \mathbf{R}$	Time.
$\mathbf{u} \in \mathbf{H}^{n_u}$	Control input variables in

¹ Grad. stud., Univ. of Michigan (UM) & intern, United Tech. Res. Center (UTRC).

² Research eng., UTRC.

³ Prof., UM.

	differential algebraic equation-based elevator model.
$v(x,t)$	Velocity of rope material (depends on both time and the position along the rope).
$x, dx \in \mathbf{R}$	Position & length of infinitesimal rope segment.
$\mathbf{x}_c \in \mathbf{R}^{n_c}, n_c$	Vector of adaptive controller design variables and its dimension.
$\mathbf{x}_e \in \mathbf{R}^{n_{xe}}$	Exogenous variables (cab mass).
$\mathbf{x}_p \in \mathbf{R}^{n_{sp}}$	Plant design variables.
$\mathbf{x}_{p,\min}, \mathbf{x}_{p,\max} \in \mathbf{R}^{x_p}$	Lower and upper bounds on plant design variables.
$\mathbf{x} \equiv \begin{bmatrix} \mathbf{x}_p^T & \mathbf{x}_c^T \end{bmatrix}^T$	Vector of system (i.e. both plant and controller) design variables.
\mathbf{X}	Set of feasible system designs.
$\mathbf{X}_p \equiv \left\{ \mathbf{x}_p : \exists \mathbf{x}_c, \begin{bmatrix} \mathbf{x}_p^T & \mathbf{x}_c^T \end{bmatrix}^T \in \mathbf{X} \right\}$	Set of feasible plant designs (projection of \mathbf{X} onto plant design vector space).
$\mathbf{X}_c(\mathbf{x}_p) \equiv \left\{ \mathbf{x}_c : \begin{bmatrix} \mathbf{x}_p^T & \mathbf{x}_c^T \end{bmatrix}^T \in \mathbf{X} \right\}$	Set of feasible controller designs for a given plant (projection of \mathbf{X} onto controller design space for \mathbf{x}_p)
$\mathbf{X}_e, \mathbf{Z}_r^o$	Sets of possible values for the exogenous variables and linearization point.
$V(x,t)$	Velocity of moving & shrinking pipe used to model the rope segment.
$\mathbf{v} \in \mathbf{H}^{n_v}$	Noises affecting differential algebraic equation-based elevator model.
$\mathbf{w} \in \mathbf{H}^{n_w}$	Disturbance signals affecting differential algebraic equation-based elevator model.
$\mathbf{y} \in \mathbf{H}^{n_y}$	Outputs of differential algebraic equation-based model.
$\mathbf{z} \in \mathbf{H}^{n_z}$	State variables of differential algebraic equation-based elevator model.
$\mathbf{z}_r, \mathbf{z}_r^o \in \mathbf{H}^{n_{zr}}$	Reduced-index states and their reference values.
$\mathbf{Z}_r, \mathbf{U}, \mathbf{W}, \mathbf{V}, \mathbf{Y}$	Deviations of $\mathbf{z}, \mathbf{u}, \mathbf{w}, \mathbf{v}$ and \mathbf{y} from linearization point.
$\mathbf{Z}_{re} \in \mathbf{H}^{n_{zr}}$	Estimates of reduced-index states.
$\sigma(x,t), \epsilon(x,t)$	Rope stress and strain
$\rho, \kappa, \beta \in \mathbf{R}$	Mass, stiffness and viscous damping coefficient of unit length of one rope.

2. MODEL CONSTRUCTION

A typical elevator with “2-to-1” roping (Fig. 1) is modeled using an object-oriented modeling language (Modelica [7-9]) that allows system-level differential algebraic equations (DAEs) to be readily assembled from component DAE models, most of which (e.g. spring and motor models) are packaged in an existing standard library [7-9]. This standard library lacks a rope model, however. Consider, therefore, the dynamics of an elevator’s rope.

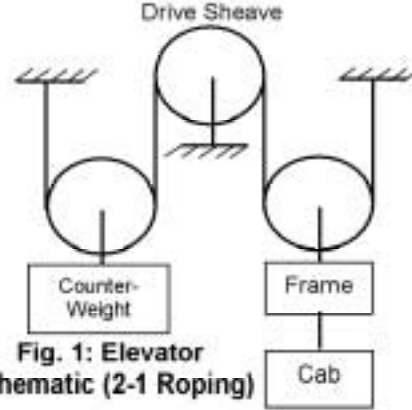


Fig. 1: Elevator Schematic (2-1 Roping)

Examine the elevator schematic in Fig. 1. As the passenger cab climbs and descends, the length of the rope segment connecting it to the drive sheave changes. Furthermore, at any given rope-sheave contact, the local velocities of the rope and sheave in contact with it are unequal. For these two reasons, the analogy of a moving and shrinking pipe is needed for modeling an elevator’s roping. Using this analogy, the lines segment connecting the two ends of a straight rope will be treated as a pipe. Let the length of the pipe be $L \in \mathbf{R}$ (where \mathbf{R} is the set of real numbers) and let the unit vector along its length be $\mathbf{s} \in \mathbf{R}^3$. Consider a segment of this rope whose endpoints are originally located at distances $x \in \mathbf{R}$ and $x+dx \in \mathbf{R}$ from one of the pipe’s endpoints. Let the components of the velocity of the pipe at x in the direction of \mathbf{s} be $V(x,t)$. Using the moving pipe analogy, the material comprising the rope can now be treated as a viscoelastic fluid flowing inside the pipe. Let the component of the velocity of the rope material at x in the direction of \mathbf{s} be $v(x,t)$. Sketching the free-body diagram of this pipe segment gives

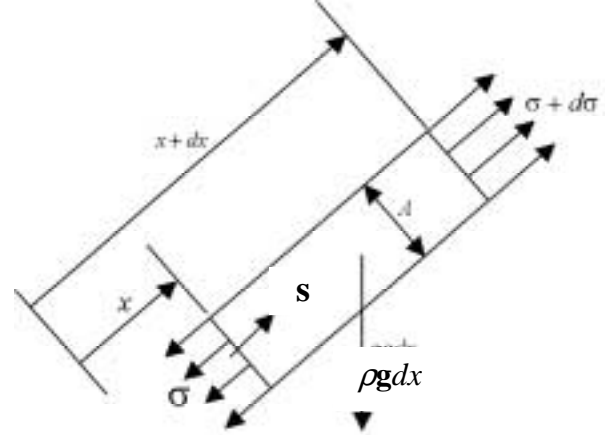


Fig. 2: Rope Free-Body Diagram

Using the momentum principle to write the equation of motion for this infinitesimal segment, eliminating higher-order terms, introducing the rope's viscoelastic properties and simplifying gives the partial differential equation (PDE)

$$\kappa \frac{\partial \varepsilon}{\partial x} + \beta \frac{\partial^2 v}{\partial x^2} = \rho \left[\frac{\partial v}{\partial t} + v \frac{\partial v}{\partial x} + V \frac{\partial v}{\partial x} - 2v \frac{dv}{dx} + \mathbf{s} \cdot \mathbf{g} \right] \quad (1)$$

where $\varepsilon(x,t)$ is the strain in the rope bundle and $\rho \in \mathbf{R}$, $\kappa \in \mathbf{R}$ and $\beta \in \mathbf{R}$ are the mass, stiffness and viscous damping coefficient of a unit length of one rope. A discretized form of this PDE, together with its appropriate boundary conditions, was programmed as a rope module in the modeling language Modelica [7-9].

The various elevator component models were visually assembled into the system model depicted in Fig. 3. This visual assembly process grouped the component DAE models into a system DAE model of the form

$$\dot{\mathbf{z}} = \mathbf{f}_z(\mathbf{z}, \mathbf{u}, \mathbf{w}, \mathbf{x}_p, \mathbf{x}_e), \mathbf{g}_z(\mathbf{z}, \mathbf{x}_p, \mathbf{x}_e) = \mathbf{0}, \mathbf{y} = \mathbf{g}_y(\mathbf{z}, \mathbf{u}, \mathbf{v}, \mathbf{x}_p, \mathbf{x}_e) \quad (2)$$

where $\mathbf{z} \in \mathbf{H}^{n_z}$, $\mathbf{u} \in \mathbf{H}^{n_u}$, $\mathbf{w} \in \mathbf{H}^{n_w}$, $\mathbf{v} \in \mathbf{H}^{n_v}$, $\mathbf{y} \in \mathbf{H}^{n_y}$, $\mathbf{x}_p \in \mathbf{R}^{n_{xp}}$ and $\mathbf{x}_e \in \mathbf{R}^{n_{xe}}$ are the vectors of states, inputs, disturbances, noises, outputs, plant design variables and exogenous variables (e.g., cab mass), respectively. The symbol \mathbf{H} denotes the Hilbert space of scalar real functions of time, and n_z , n_u , n_w , n_v , n_y , n_{xp} and n_{xe} are the (integer) numbers of states, inputs, disturbances, noises, outputs, plant design variables and exogenous variables, respectively.

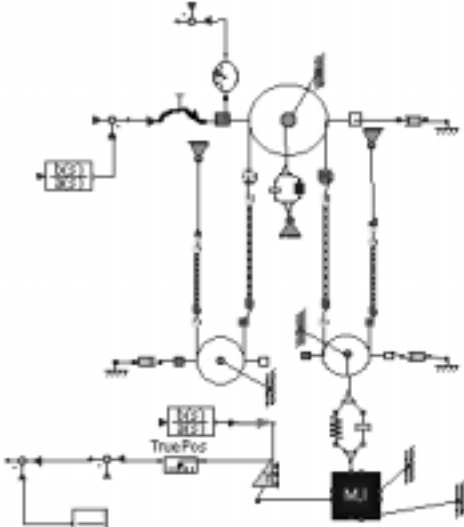


Fig. 3: Open-loop Elevator Model

DAE models, despite their generality, are not directly conducive to control system design and so an index reduction is carried out to convert the elevator's model into the more desirable ordinary differential equation (ODE) form below

$$\dot{\mathbf{z}}_r = \mathbf{f}_{z_r}(\mathbf{z}_r, \mathbf{u}, \mathbf{w}, \mathbf{x}_p, \mathbf{x}_e), \mathbf{y} = \mathbf{g}_{y_r}(\mathbf{z}_r, \mathbf{u}, \mathbf{v}, \mathbf{x}_p, \mathbf{x}_e) \quad (3)$$

where $\mathbf{z}_r \in \mathbf{H}^{n_{z_r}}$ denotes the state variables remaining after index reduction (and n_{z_r} is the order of the reduced-index dynamic model). Typically, the ODE-based model for an elevator depends on the cab mass (an exogenous variable) and height (a state variable), and is

hence nonlinear. To simplify the design of an elevator's controller, its ODE model can be linearized about some state $\mathbf{z}_r^o \in \mathbf{H}^{n_{z_r}}$ to give

$$\dot{\mathbf{Z}}_r = \mathbf{A}\mathbf{Z}_r + \mathbf{B}\mathbf{U} + \mathbf{G}\mathbf{W}, \mathbf{Y} = \mathbf{C}\mathbf{Z}_r + \mathbf{D}\mathbf{U} + \mathbf{V} \quad (4)$$

where capitalization indicates deviation from the linearization point and the matrices $\mathbf{A} \in \mathbf{R}^{n_{z_r} \times n_{z_r}}$, $\mathbf{B} \in \mathbf{R}^{n_{z_r} \times n_u}$, $\mathbf{G} \in \mathbf{R}^{n_{z_r} \times n_w}$, $\mathbf{C} \in \mathbf{R}^{n_y \times n_{z_r}}$ and $\mathbf{D} \in \mathbf{R}^{n_y \times n_u}$ depend on the variables \mathbf{x}_p , \mathbf{x}_e and \mathbf{z}_r^o . A family of linearized models is thus created corresponding to different values of \mathbf{x}_e and \mathbf{z}_r^o (i.e., the cab mass and height) for every plant design \mathbf{x}_p .

The two primary sources of vibration in a typical elevator with 2-to-1 roping are the driving motor's output torque ripple and the vertical friction forces from the guide rails. These disturbances are colored, low-frequency random signals, as opposed to the noises in the two feedback measurements (drive sheave angle and cab height), which occur at higher frequencies. Linear Quadratic Gaussian (LQG) control [10] is used here to trade off the two conflicting requirements of disturbance rejection and noise attenuation. Since LQG design assumes white random signals, first-order filters have been incorporated in the elevator model in Fig. 3 and Eq. (4) to color the disturbances and noises before injecting them into the plant model.

3. THE SYSTEM OPTIMIZATION PROBLEM

In this section, the combined plant/controller optimization is posed. In Section 4 the problem is solved both sequentially and simultaneously the results are compared. Since passenger acceleration is a good measure of ride discomfort, a reasonable optimization goal is to minimize the passenger acceleration while keeping the required control input low. The optimization objective is then formulated as

$$J = \mathbb{E} \int_0^{\infty} (a^2 + \mathbf{R}\mathbf{U}^T \mathbf{U}) dt = \mathbb{E} \int_0^{\infty} (\mathbf{Z}_r^T \mathbf{C}_a^T \mathbf{C}_a \mathbf{Z}_r + \mathbf{R}\mathbf{U}^T \mathbf{U}) dt \quad (5)$$

where \mathbb{E} is the expectation operator, $\mathbf{U} \in \mathbf{H}^{n_u}$ is the drive motor's input voltage, and the passenger acceleration $a \in \mathbf{H}$ is related to the state vector by:

$$a = \mathbf{C}_a(\mathbf{x}_p, \mathbf{z}_r^o, \mathbf{x}_e) \mathbf{Z}_r \quad (6)$$

Passenger cab vibrations can be reduced by correctly designing the counter-weight, ropes, isolation pads, and isolation hitches. Altogether, there are 19 plant design variables (e.g., rope and isolation pad stiffnesses) comprising the vector \mathbf{x}_p . They are constrained by upper and lower bounds denoted by $\mathbf{x}_{p,\max}$ and $\mathbf{x}_{p,\min}$, respectively, reflecting constraints on strength and static deflection.

For a given elevator plant design, vibrations can be further reduced using active control. Specifically, one can significantly reduce the cost function in Eq. (5) by measuring the passenger cab's vertical velocity and the drive sheave's angular velocity, feeding these two (noisy) measurements into a state filter to

estimate the remaining elevator states and then using full feedback of the estimated states to generate the drive motor's input voltage. The gains \mathbf{L} and \mathbf{K} of the filter and the controller can be found by solving the following LQG problem [10]:

$$\min_{\mathbf{K}, \mathbf{L}} E \int_0^{\infty} (\mathbf{Z}_r^T \mathbf{C}_a^T \mathbf{C}_a \mathbf{Z}_r + \mathbf{R} \mathbf{U}^T \mathbf{U}) dt$$

subject to:

$$\begin{aligned} \dot{\mathbf{Z}}_r &= \mathbf{A} \mathbf{Z}_r + \mathbf{B} \mathbf{U} + \mathbf{G} \mathbf{W}, \quad \mathbf{Y} = \mathbf{C} \mathbf{Z}_r + \mathbf{D} \mathbf{U} + \mathbf{V}, \quad \mathbf{A} = \mathbf{A}(\mathbf{x}_p; \mathbf{z}_r^o, \mathbf{x}_e), \\ \mathbf{B} &= \mathbf{B}(\mathbf{x}_p; \mathbf{z}_r^o, \mathbf{x}_e), \quad \mathbf{G} = \mathbf{G}(\mathbf{x}_p; \mathbf{z}_r^o, \mathbf{x}_e), \quad \mathbf{C} = \mathbf{C}(\mathbf{x}_p; \mathbf{z}_r^o, \mathbf{x}_e), \\ \mathbf{D} &= \mathbf{D}(\mathbf{x}_p; \mathbf{z}_r^o, \mathbf{x}_e), \quad \mathbf{C}_a = \mathbf{C}_a(\mathbf{x}_p; \mathbf{z}_r^o, \mathbf{x}_e), \quad E(\mathbf{W}^T \mathbf{W}) = \mathbf{E}_W, \end{aligned} \quad (7)$$

$E(\mathbf{V}^T \mathbf{V}) = \mathbf{E}_V$, $\dot{\mathbf{Z}}_{re} = \mathbf{A} \mathbf{Z}_{re} + \mathbf{B} \mathbf{U} + \mathbf{L}(\mathbf{Y} - \mathbf{C} \mathbf{Z}_{re})$, $\mathbf{U} = -\mathbf{K} \mathbf{Z}_{re}$ where $\mathbf{E}_W \in \mathbf{R}^{n_w \times n_w}$ and $\mathbf{E}_V \in \mathbf{R}^{n_v \times n_v}$ are the disturbance and noise covariances, $\mathbf{Z}_{re} \in \mathbf{H}^{n_r}$ is the vector of state estimates, and $\mathbf{K} \in \mathbf{R}^{n_u \times n_r}$ and $\mathbf{L} \in \mathbf{R}^{n_z \times n_y}$ are the LQG feedback and estimation gains, respectively.

The solution of the above LQG problem depends not only on the plant design \mathbf{x}_p but also on the cab mass \mathbf{x}_e and the linearization point \mathbf{z}_r^o . Therefore, for every given elevator plant design, one can determine a family or gain schedule [11] of LQG controllers corresponding to the various possible cab masses and heights. Should one utilize this entire gain schedule for vibration reduction, or should a single representative set of gains from this schedule be used?

To answer this question, consider a typical elevator plant and two different disturbance profiles that may act on this plant. The dominant disturbance source in the first, the rail irregularity case (RIC), is the irregular vertical friction force between the cab and guide rails and in the second, the torque ripple case (TRC), is the drive motor's output torque ripple. An LQG controller was designed for this plant for each of these two disturbance profiles assuming a half-full cab at mid-rise. Figures 4 and 5 show how the objective function (from Eq. 5) for the elevator plant and each of the two controllers varies with the cab's normalized mass and height.

Fig. 4: Contours of the Performance Function, J , with Respect to Normalized Cab Mass and Normalized Distance to Drive Sheave, Rail Irregularity Case

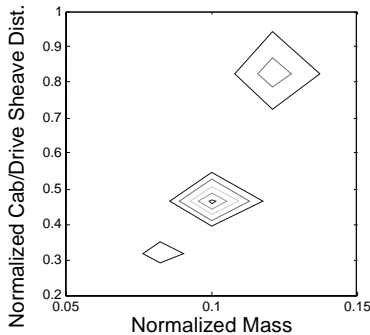


Fig. 5: Contours of the Performance Function, J , with Respect to the Normalized Cab Mass and Normalized Distance to Drive Sheave – Torque Ripple Case

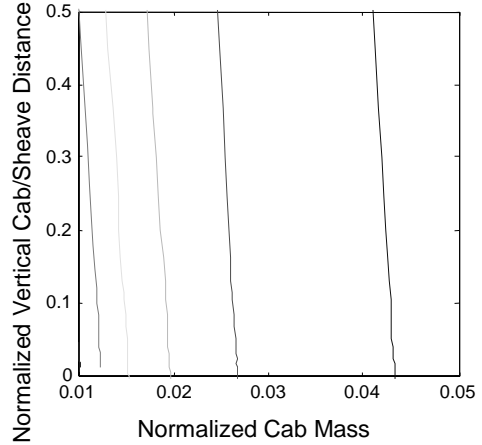


Figure 4 shows that the vibrations excited by the guide rail irregularity increase significantly at those cab masses and heights where the elevator's resonance frequencies and the disturbance frequencies meet. Three modes appear in the figure, the first two of which are typically important in practical applications. In the first, "bounce" mode, the cab and counterweight bounce on their respective ropes, with very little drive sheave motion. Because of the small drive sheave motion associated with it, this bounce mode tends to be more difficult to control than the second, "sheave" mode, in which the cab and counterweight undergo out-of-phase oscillations and the sheave also vibrates significantly.

Figure 5 shows that, like the rail irregularity-induced vibrations, the vibrations induced by the torque ripple also vary with the cab mass and height, but the nature of the variation is simpler. The worst-case torque ripple-induced vibrations occur when the passenger cab is at the top floor and has the minimum possible mass (i.e., no passengers). This observation agrees with practical experience.

To summarize, in both the RIC and TRC, the worst-case vibrations are greater than the vibrations at the typical values of the cab height and mass used for LQG control design. The difference is quite significant. In fact, the worst-case values of the objective function in Eq. (5) are 9923 and 2041 times greater than the values corresponding to the nominal cab mass and height for the RIC and TRC, respectively. When the LQG gains are scheduled versus the cab mass and height, the worst-case magnitudes of the cost function become only 1240 and 1.1017 times the typical values for the RIC and TRC, respectively. Thus, scheduling the LQG gains versus the cab mass and height is very beneficial because it reduces the worst-case vibrations drastically.

We now proceed to find a plant and an LQG gain schedule which, together, yield the most comfortable worst-case ride. This plant/controller pair will be the solution to the system-level

mini-max4 optimization problem stated below. The objective is to minimize the worst-case value of the function in Eq. (5), and the variables and constraints include both plant and controller variables and constraints.

$$\min_{\mathbf{x}_p, \mathbf{K}(\mathbf{x}_e, \mathbf{z}_r^o), \mathbf{L}(\mathbf{x}_e, \mathbf{z}_r^o)} \max_{\mathbf{x}_e, \mathbf{z}_r^o} \mathbb{E} \int_0^{\infty} (\mathbf{z}_r^T \mathbf{C}_a^T \mathbf{C}_a \mathbf{z}_r + \mathbf{R} \mathbf{U}^T \mathbf{U}) dt$$

subject to:

$$\mathbf{x}_{p, \min} \leq \mathbf{x}_p \leq \mathbf{x}_{p, \max},$$

$$\dot{\mathbf{Z}}_r = \mathbf{A} \mathbf{Z}_r + \mathbf{B} \mathbf{U} + \mathbf{G} \mathbf{W}, \quad \mathbf{Y} = \mathbf{C} \mathbf{Z}_r + \mathbf{D} \mathbf{U} + \mathbf{V}, \quad \mathbf{A} = \mathbf{A}(\mathbf{x}_p; \mathbf{z}_r^o, \mathbf{x}_e),$$

$$\mathbf{B} = \mathbf{B}(\mathbf{x}_p; \mathbf{z}_r^o, \mathbf{x}_e), \quad \mathbf{G} = \mathbf{G}(\mathbf{x}_p; \mathbf{z}_r^o, \mathbf{x}_e), \quad \mathbf{C} = \mathbf{C}(\mathbf{x}_p; \mathbf{z}_r^o, \mathbf{x}_e),$$

$$\mathbf{D} = \mathbf{D}(\mathbf{x}_p; \mathbf{z}_r^o, \mathbf{x}_e), \quad \mathbf{C}_a = \mathbf{C}_a(\mathbf{x}_p; \mathbf{z}_r^o, \mathbf{x}_e), \quad \mathbf{E}(\mathbf{W}^T \mathbf{W}) = \mathbf{E}_W,$$

$$\mathbf{E}(\mathbf{V}^T \mathbf{V}) = \mathbf{E}_V, \quad (8)$$

$$\dot{\mathbf{Z}}_{re} = \mathbf{A} \mathbf{Z}_{re} + \mathbf{B} \mathbf{U} + \mathbf{L}(\mathbf{Y} - \mathbf{C} \mathbf{Z}_{re}), \quad \mathbf{U} = -\mathbf{K} \mathbf{Z}_{re}$$

Note that the LQG gains \mathbf{K} and \mathbf{L} are no longer constant, but rather dependent on the exogenous variables \mathbf{x}_e and the linearization point \mathbf{z}_r^o , since the controller is now gain-scheduled. The next section shows how this optimization problem is solved.

4. NESTED PLANT/CONTROLLER OPTIMIZATION

Several strategies exist in the literature for solving combined plant/controller optimization problems such as in Eq. (8) [12]. *Sequential optimization* partitions a given combined problem into plant and controller optimization subproblems that are then solved in tandem. *Simultaneous, or combined, optimization*, optimizes all the components of a given system together. Simultaneous optimization guarantees system-level optimality, while sequential optimization does not. Unfortunately, simultaneous optimization does not take advantage of the fact that the control optimization subproblem (e.g. the LQG optimization subproblem) of a system-level optimization problem often has known analytic solutions. *Nested optimization* is a strategy that both takes advantage of this fact and guarantees system-level optimality [12].

In nested plant/controller optimization, the system-level objective is optimized with respect to the plant design, implicitly assuming the optimal controller for the plant. This produces a two-loop nested process: the outer loop optimizes the system objective with respect to the plant, and the inner loop generates the optimal controller for every plant computed by the outer loop (see Fig. 6). Under the special assumption that the combined space of feasible plants and controllers can be projected *a priori* onto the plant design vector space, nested optimization guarantees system-level optimality [12]. Furthermore, the inner loop in nested optimization is a controller optimization subproblem and can be solved using optimal control theory.

⁴ The minimization is carried out with respect to all the plant and control design variables, while the maximization is carried out with respect to the exogenous variables \mathbf{x}_e and the linearization point \mathbf{z}_r^o to find the worst-case ride.

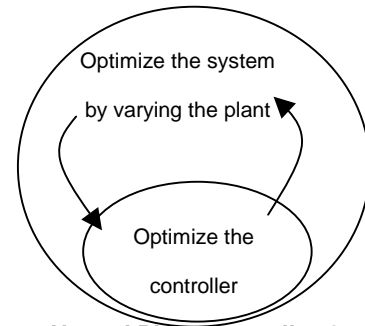


Fig. 6: Nested Plant/Controller Optimization

Nested optimization, as defined in [12], is applicable to LTI systems, as opposed to systems that employ adaptive control [11]. However, it is possible to extend nested optimization to adaptive systems (including gain-scheduled systems) where the control gains vary with time without losing the system-level optimality guarantee, as we show below.

Theorem 1: Denote the vector of adaptive controller design variables by $\mathbf{x}_c \in \mathbf{R}^{n_c}$, and note that this vector is time-invariant for a given adaptive controller design (i.e. even though the instantaneous control gains \mathbf{K} and \mathbf{L} vary with time for a given adaptive controller design, \mathbf{x}_c does not). For the elevator optimization problem in Eq. (8), \mathbf{x}_c

represents the entire LQG gain schedule. Now let $\mathbf{x} = [\mathbf{x}_p^T \quad \mathbf{x}_c^T]^T$ be the vector of system design variables, let the set of feasible system designs be \mathbf{X} , assume that the sets of possible values of the exogenous variables (\mathbf{x}_e) and linearization points (\mathbf{z}_r^o) are \mathbf{X}_e and \mathbf{Z}_r^o , respectively, and consider the system optimization problem:

$$\mathbf{x}^* = \arg \min_{\mathbf{x} \in \mathbf{X}} \max_{\mathbf{x}_e \in \mathbf{X}_e, \mathbf{z}_r^o \in \mathbf{Z}_r^o} f(\mathbf{x}, \mathbf{x}_e, \mathbf{z}_r^o) \quad (9)$$

where $f(\mathbf{x}, \mathbf{x}_e, \mathbf{z}_r^o)$ is the scalar system optimization objective (for the elevator optimization problem in Eq. (8), $f(\mathbf{x}, \mathbf{x}_e, \mathbf{z}_r^o)$ is the objective function J). Let the set of feasible plant designs \mathbf{X}_p be the projection of the set of feasible system designs onto the plant design vector space, and let the set of feasible controller designs for a given plant $\mathbf{X}_c(\mathbf{x}_p)$ be the projection of the set of feasible systems onto the controller design vector space for a given plant, i.e.,

$$\mathbf{X}_p \equiv \left\{ \mathbf{x}_p : \exists \mathbf{x}_c, [\mathbf{x}_p^T \quad \mathbf{x}_c^T]^T \in \mathbf{X} \right\} \quad (10)$$

$$\mathbf{X}_c(\mathbf{x}_p) \equiv \left\{ \mathbf{x}_c : [\mathbf{x}_p^T \quad \mathbf{x}_c^T]^T \in \mathbf{X} \right\} \quad (11)$$

Then the solution to the following three-loop nested optimization problem is a system optimum and satisfies Eq. (9):

$$\text{Outer loop: } \mathbf{x}_p^* = \arg \min_{\mathbf{x}_p \in \mathbf{X}_p} f([\mathbf{x}_p^T \quad (\mathbf{x}_c^*)^T]^T, \mathbf{x}_e^*, \mathbf{z}_r^{o*}) \quad (12)$$

$$\text{Intermediate loop: } \mathbf{x}_c^* = \arg \min_{\mathbf{x}_c \in \mathbf{X}_c(\mathbf{x}_p)} f([\mathbf{x}_p^T \quad \mathbf{x}_c^T]^T, \mathbf{x}_e^*, \mathbf{z}_r^{o*}) \quad (13)$$

$$\text{Inner loop: } (\mathbf{x}_e^*, \mathbf{z}_r^{o*}) = \arg \max_{\mathbf{x}_e \in \mathbf{X}_e, \mathbf{z}_r^o \in \mathbf{Z}_r^o} f([\mathbf{x}_p^T \quad \mathbf{x}_c^T]^T, \mathbf{x}_e, \mathbf{z}_r^o) \quad (14)$$

The proof follows directly from the definition of a minimum and is omitted for brevity ◀

Note that the above nested optimization strategy (Eq. (12-14)) can only be used if one can determine the set \mathbf{X}_p a priori. In other words, nested optimization can only proceed if the projection of the set of feasible systems onto the plant design space is known [12]. Furthermore, note that this nested optimization strategy (Eq. (12-14))

does not assume a specific adaptive control law and can hence be used regardless of whether the controller is gain-scheduled, self-tuning, model-predictive, etc. For the combined plant/gain-scheduled LQG controller problem in Eq. (8), Eq. (12-14) become:

$$\begin{aligned} \text{Outer loop: } \min_{\mathbf{x}_p} & \int_0^{\infty} \left(\mathbf{Z}_r^* T \mathbf{C}_a^* T \mathbf{C}_a^* \mathbf{Z}_r^* + \mathbf{R} \mathbf{U}^{*T} \mathbf{U}^* \right) dt \\ \text{subject to:} & \\ \mathbf{x}_{p,\min} & \leq \mathbf{x}_p \leq \mathbf{x}_{p,\max}, \quad \mathbf{C}_a^* = \mathbf{C}_a(\mathbf{x}_p; \mathbf{z}_r^*, \mathbf{x}_e^*) \\ \mathbf{Z}_r^*, \mathbf{U}^* & = \text{outputs of intermediate loop corresponding to} \\ & \text{the values of } \mathbf{x}_e \text{ and } \mathbf{z}_r^o \text{ computed by inner loop} \end{aligned} \quad (15)$$

Intermediate loop:

Find the gain schedules $\mathbf{K}^*(\mathbf{x}_e, \mathbf{z}_r^o)$ and $\mathbf{L}^*(\mathbf{x}_e, \mathbf{z}_r^o)$ such that, for every $\mathbf{x}_e \in \mathbf{X}_e$ and $\mathbf{z}_r^o \in \mathbf{Z}_r^o$:

$$\begin{aligned} \left(\mathbf{K}^*(\mathbf{x}_e, \mathbf{z}_r^o), \mathbf{L}^*(\mathbf{x}_e, \mathbf{z}_r^o) \right) & = \arg \min_{\mathbf{K}, \mathbf{L}} \int_0^{\infty} \left(\mathbf{Z}_r^T \mathbf{C}_a^T \mathbf{C}_a \mathbf{Z}_r + \mathbf{R} \mathbf{U}^T \mathbf{U} \right) dt \\ \text{subject to:} & \\ \dot{\mathbf{Z}}_r & = \mathbf{A} \mathbf{Z}_r + \mathbf{B} \mathbf{U} + \mathbf{G} \mathbf{W}, \quad \mathbf{Y} = \mathbf{C} \mathbf{Z}_r + \mathbf{D} \mathbf{U} + \mathbf{V}, \quad \mathbf{A} = \mathbf{A}(\mathbf{x}_p; \mathbf{z}_r^o, \mathbf{x}_e), \\ \mathbf{B} & = \mathbf{B}(\mathbf{x}_p; \mathbf{z}_r^o, \mathbf{x}_e), \quad \mathbf{G} = \mathbf{G}(\mathbf{x}_p; \mathbf{z}_r^o, \mathbf{x}_e), \quad \mathbf{C} = \mathbf{C}(\mathbf{x}_p; \mathbf{z}_r^o, \mathbf{x}_e), \\ \mathbf{D} & = \mathbf{D}(\mathbf{x}_p; \mathbf{z}_r^o, \mathbf{x}_e), \quad \mathbf{C}_a = \mathbf{C}_a(\mathbf{x}_p; \mathbf{z}_r^o, \mathbf{x}_e), \quad \mathbf{E}(\mathbf{W}^T \mathbf{W}) = \mathbf{E}_W, \\ \mathbf{E}(\mathbf{V}^T \mathbf{V}) & = \mathbf{E}_V, \\ \dot{\mathbf{Z}}_{re} & = \mathbf{A} \mathbf{Z}_{re} + \mathbf{B} \mathbf{U} + \mathbf{L}(\mathbf{Y} - \mathbf{C} \mathbf{Z}_{re}), \quad \mathbf{U} = -\mathbf{K} \mathbf{Z}_{re} \end{aligned} \quad (16)$$

$$\begin{aligned} \text{Inner Loop: } \max_{\mathbf{x}_e \in \mathbf{X}_e, \mathbf{z}_r^o \in \mathbf{Z}_r^o} & \int_0^{\infty} \left(\mathbf{Z}_r^T \mathbf{C}_a^T \mathbf{C}_a \mathbf{Z}_r + \mathbf{R} \mathbf{U}^T \mathbf{U} \right) dt \\ \text{subject to:} & \\ \dot{\mathbf{Z}}_r & = \mathbf{A} \mathbf{Z}_r + \mathbf{B} \mathbf{U} + \mathbf{G} \mathbf{W}, \quad \mathbf{Y} = \mathbf{C} \mathbf{Z}_r + \mathbf{D} \mathbf{U} + \mathbf{V}, \\ \mathbf{A} & = \mathbf{A}(\mathbf{x}_p; \mathbf{z}_r^o, \mathbf{x}_e), \quad \mathbf{B} = \mathbf{B}(\mathbf{x}_p; \mathbf{z}_r^o, \mathbf{x}_e), \\ \mathbf{G} & = \mathbf{G}(\mathbf{x}_p; \mathbf{z}_r^o, \mathbf{x}_e), \quad \mathbf{C} = \mathbf{C}(\mathbf{x}_p; \mathbf{z}_r^o, \mathbf{x}_e), \\ \mathbf{D} & = \mathbf{D}(\mathbf{x}_p; \mathbf{z}_r^o, \mathbf{x}_e), \quad \mathbf{C}_a = \mathbf{C}_a(\mathbf{x}_p; \mathbf{z}_r^o, \mathbf{x}_e), \\ \mathbf{E}(\mathbf{W}^T \mathbf{W}) & = \mathbf{E}_W, \quad \mathbf{E}(\mathbf{V}^T \mathbf{V}) = \mathbf{E}_V, \\ \dot{\mathbf{Z}}_{re} & = \mathbf{A} \mathbf{Z}_{re} + \mathbf{B} \mathbf{U} + \mathbf{L}(\mathbf{Y} - \mathbf{C} \mathbf{Z}_{re}), \quad \mathbf{U} = -\mathbf{K} \mathbf{Z}_{re} \end{aligned} \quad (17)$$

For each of the two disturbance profiles presented in Section 3 (namely the RIC and TRC), sequential optimization was used to find the plant with minimal worst-case open-loop vibrations and the controller which, for that plant, minimizes the worst-case closed-loop vibrations. Using the two resulting system designs as initial guesses, the above three-loop nested optimization strategy was employed to find the truly optimal combined plant/controller designs.

In the rail irregularity case (RIC), nested optimization found a new plant/controller pair exhibiting a worst-case value of the cost function that is 52% less than that obtained using sequential optimization. In the torque ripple case (TRC), however, nested optimization produced a system design identical to that produced by sequential plant/adaptive LQG controller optimization.

The combined plant/controller optimization literature states that the plant and controller optimization problems are generally coupled in the sense that their sequential solution does not always furnish

system optima [1-6]. Here we presented two optimization problems that differ only by the nature of the external disturbance profile. Why, then, did only one of these problems exhibit the plant/controller optimization “coupling”?

The answer lies in the relative physical locations of the dominant disturbance source, sensors and actuators. In both the TRC and RIC, a better passive design is one incorporating more “compliance”. The difference between the two cases, however, is that this additional compliance physically isolates the drive sheave (where both the control torque is applied and one of the two feedback measurements is made) from the disturbance source in the RIC (where the disturbance acts on the cab) but not in the TRC (where the disturbance acts on the drive sheave). Therefore, the elevator plant and controller optimization problems presented herein are coupled only when the dominant source is the rail irregularity, because it is only in that case that the increased plant compliance reduces the controller’s authority over the vibrations. This can be seen from Figures 7-9⁵. Figures 7 and 8 show the open-loop frequency response of the passenger acceleration to the rail disturbance force and the motor’s input torque for the sequentially optimized and system-optimal designs for the RIC. Figure 9 compares the closed-loop frequency response of the passenger acceleration to the rail irregularity for the sequentially optimized and system-optimal designs for the RIC.

Fig. 7: Open-Loop Effect of Rail Irregularity on Passenger Acceleration, RIC

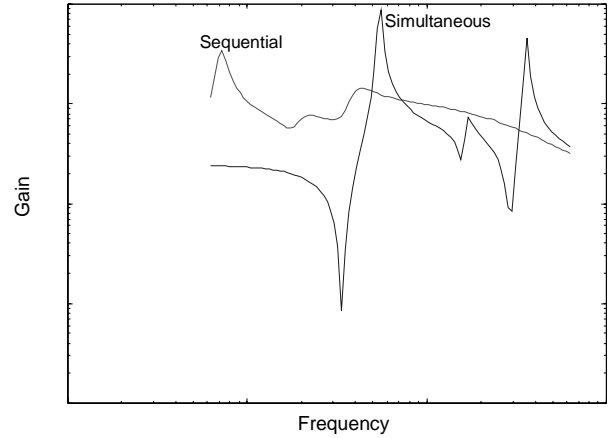
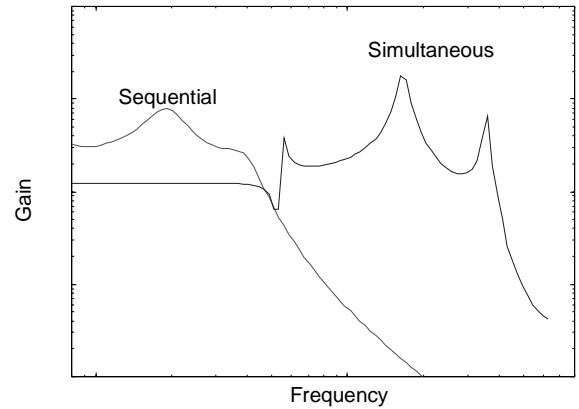


Fig. 8: Open-Loop Effect of Control Torque on Passenger Acceleration, RIC



⁵ Axis numbering is omitted from Figures 7-9 to preserve the research sponsor’s rights (see section 7).

Fig. 9: Closed-Loop Effect of Rail Irregularity on Passenger Acceleration, RIC

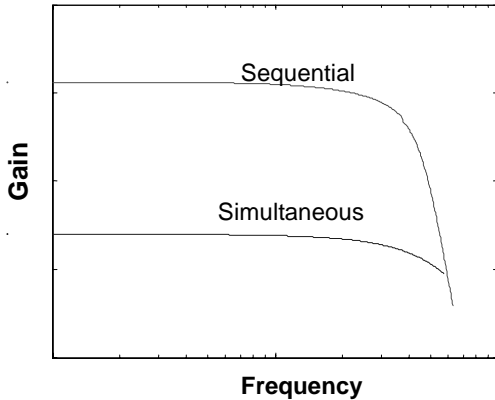


Figure 7 shows that sequential optimization produces a plant with lower open-loop resonance frequencies and resonant peaks than the system-optimal plant. Therefore, sequential optimization produces a better passive design than nested optimization. Better passive vibration isolation, however, comes at the expense of less control authority over the vibrations. As Figure 8 shows, the sequentially optimized plant has a much smaller bandwidth over the motor's torque can affect the cab vibrations. Nested optimization, on the other hand, produces an elevator plant which, though suboptimal with respect to passive vibration isolation, is easier to control. Consequently, when the optimal controller is added to each of the sequentially optimized and system-optimal plants, the latter plant exhibits a lower closed-loop frequency response to the rail irregularity, as Fig. 9 reveals.

In conclusion, therefore, depending on the relative physical locations of an elevator's sensors, actuators and disturbance source, better passive vibration isolation may reduce the controller's authority over the vibrations, thereby coupling the passive and active ride comfort optimization problems. When this coupling exists, combined plant/controller optimization, using the nested strategy described in Theorem 1, finds the truly optimal system design, whereas sequential optimization does not. The influence of the relative locations of an elevator's sensors, actuators and disturbance sources on the plant/controller optimization coupling is further illustrated using the simple mass-spring-mass example in Appendix A.

5. CONCLUSIONS

This paper presented the modeling and optimization of the plant and controller of an elevator for minimal vibration. The optimization was carried out for two different disturbance profiles. The dominant disturbance source was the drive motor's torque ripple in one profile and the guide rail irregularity in the second. Sequential plant/LQG control optimization was used to find benchmark designs for each of these profiles. The LQG gains were scheduled versus the cab mass and height to increase robustness. A standard nested plant/controller optimization procedure from the literature was modified for use with adaptive control, shown to find system-level optima and used to optimize the elevator's plant and gain-scheduled LQG controller. The resulting system was superior to the sequentially optimized system only when the guide rail irregularity was the dominant disturbance source, because it is only in that case that passive and active vibration isolation competed. This provides some strong insights into the coupling between the plant and controller optimization problems. Specifically, the paper has shown that this coupling depends

significantly on the relative locations of the actuators and disturbance sources. A simple example was used to illustrate this fact.

6. ACKNOWLEDGEMENTS

The authors would like to thank the United Technologies Research Center (UTRC) for sponsoring this work. In-depth numerical and modeling details are proprietary to UTRC and have been omitted from this paper.

7. REFERENCES

- 1- Reyer, J. A., 2000, "Combined Embodiment Design and Control: Effect of Cross-Disciplinary Coupling", *Ph.D. Dissertation: The University of Michigan*, 2000.
- 2- Reyer, J. A. and Papalambros, P. Y., 2000, "An Investigation into the Modeling and Solution Strategies for Optimal Design and Control", *Proceedings of the 2000 ASME Design Engineering Technical Conferences*.
- 3- Youcef-Toumi, K., 1996, "Modeling, Design, and Control Integration: A Necessary Step in Mechatronics", *Journal of Guidance, Control, and Dynamics*, vol. 20.
- 4- Reyer, J. A. and Papalambros, P. Y., 1999, "Optimal Design and Control of an Electric DC Motor", *Proceedings of the 1999 ASME Design Engineering Technical Conferences*.
- 5- Asada, H., Park, J. H. and Rai, S., 1999, "A Control-Configured Flexible Arm: Integrated Structure/Control Design", *Proceedings of the 1999 IEEE International Conference on Robotics and Automation*.
- 6- Smith, M. J., Grigoriadis, K. M. and Skelton, R. E., "The Optimal Mix of Passive and Active Control in Structures", *Journal of Guidance, Control, and Dynamics*, vol. 20.
- 7- Elmqvist, H., Mattson, S. E. and Otter, M., 1998, "Modelica – The New Object-Oriented Modeling Language", *Proceedings of the 12th European Simulation Multiconference*.
- 8- Elmqvist, H., Mattson, S. E. and Otter, M., 1999, "Modelica – A Language for Physical System Modeling, Visualization and Interaction", *Proceedings of the 1999 IEEE Symposium on Computer-Aided Control System Design*.
- 9- Astrom, K. J., Elmqvist, H. and Mattson, S. E., 1998, "Evolution of Continuous-Time Modeling and Simulation", *Proceedings of the 12th European Simulation Multiconference*.
- 10- Lewis, F. L. and Syrmos, V. L., *Optimal Control*, Wiley, 1994.
- 11- Astrom, K. J. and Wittenmark, B., *Adaptive Control*, Addison-Wesley, 1995.
- 12- Fathy, H. K., Reyer, J. A., Papalambros, P. Y. and Ulsoy, A. G., 2001, "On the Coupling between the Plant and Controller Optimization Problems", *Proceedings of the 2001 American Control Conference*.

8. APPENDIX A: TWO-MASS EXAMPLE

Consider the mass-spring-mass system in Fig. 10. Let the magnitudes of both masses be 1kg and suppose that one seeks to minimize the steady-state vibrations of mass B by varying the spring stiffness and the design of an active controller applying a force onto mass A. Let the original spring stiffness be 200kN/m, let that be the maximum permissible stiffness and let a sinusoidal external disturbance force of magnitude 1N and frequency 100Hz act on this system.

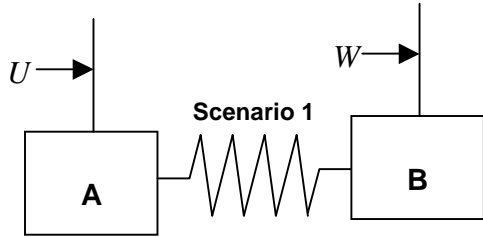
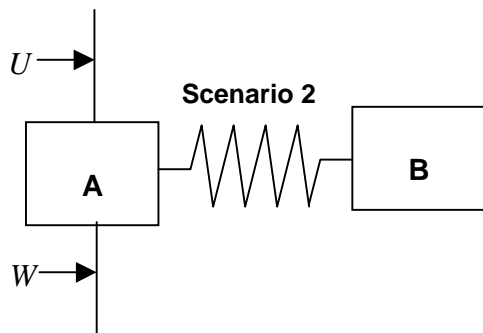


Fig. 10: Illustrative Example



Now consider two different scenarios. In the first scenario, the disturbance force acts on mass B, and in the second, it acts on mass A. Figure 11 shows that for both scenarios, the amplitude of the vibrations of mass B decreases as the spring stiffness decreases. Therefore, for both scenarios, a better passive design for vibration isolation is a more flexible one. A better passive design is not always easier to control, however. To see this, consider the open-loop gain of the transfer function from the control input to the force generated by that control input at the point where the disturbance is applied. This transfer function represents the ease with which the controller can oppose the disturbance. One can think of this transfer function as a “lever arm” from the control input to that point where the control input and disturbance “compete”⁶. Figure 12 plots the open-loop magnitude of this lever arm vs. the spring stiffness for the two scenarios at hand.

⁶ If the position of mass B, $Y(s)$, is related to the control input and disturbance force by $Y(s) = G(s)U(s)+H(s)W(s)$, then this “lever arm” equals the gain of $G(s)/H(s)$ at 100Hz.

Fig.11 : Passive Vibration Isolation

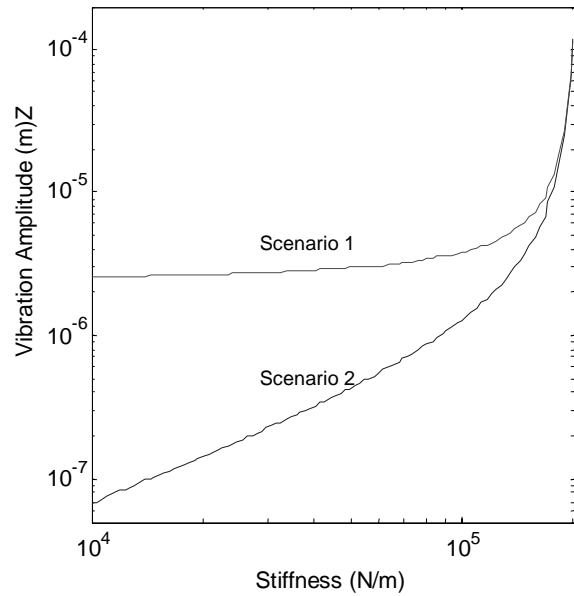


Fig.12 : Control Input "Lever Arm"

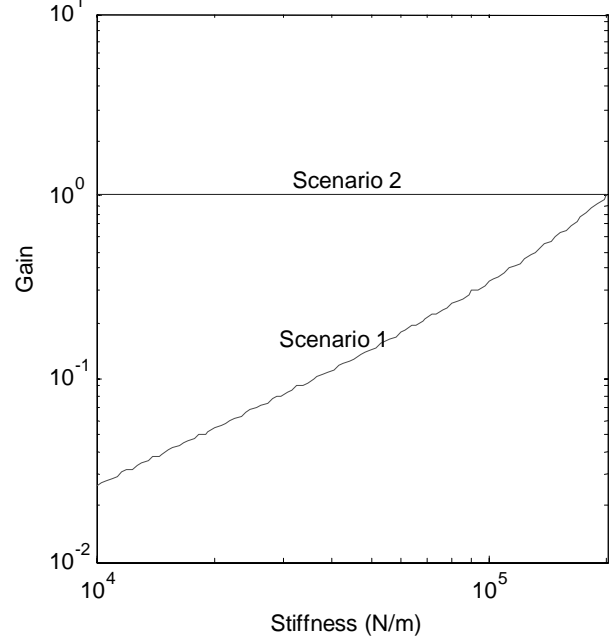


Figure 12 reveals a fundamental difference between the two optimization scenarios. In the first scenario, reducing the spring stiffness reduces the controller’s ability to oppose the disturbances. Therefore, a better passive design is also one where the controller has less authority. The plant and controller optimization problems compete in this scenario, which leads to a plant/controller optimization coupling. In the second scenario, however, reducing the spring stiffness has no influence over the controller’s ability to oppose disturbances, because both the control force and disturbance force act on the same mass. Therefore, a better passive design is not more difficult to control, and the two problems decouple.